Results in Physics 10 (2018) 10–17

Contents lists available at ScienceDirect

Results in Physics

journal homepage: www.elsevier.com/locate/rinp

MHD fractional Jeffrey's fluid flow in the presence of thermo diffusion, thermal radiation effects with first order chemical reaction and uniform heat flux

M.A. Imran[b], Fizza Miraj[b], I. Khan[a,*], I. Tlili[c]

[a] Faculty of Mathematics and Statistics, Ton Duc Thang University, Ho Chi Minh City, Viet Nam
[b] Department of Mathematics, University of Management and Technology Lahore, C-II Johar Town, Lahore 54700, Pakistan
[c] Energy and Thermal Systems Laboratory, National Engineering School of Monastir, Street Ibn El Jazzar, 5019 Monastir, Tunisia

ARTICLE INFO

Keywords:
Fractional Jeffrey's fluid
Heat flux
MHD
Heat and mass transfer
Soret effect
Chemical reaction

ABSTRACT

Exact analysis is about the natural convection flow of non-Newtonian Jeffrey fluid with the Caputo-Fabrizio fractional derivative of non-singular kernel has been discussed in this work. The Laplace transform method is used to obtain the solutions of dimensionless temperature, concentration and velocity fields with non-integer order derivative. Moreover, in the mathematical modelling of the problem, the additional effects like Soret effect, MHD, heat sink, radiations, chemical reaction, porous medium and uniform heat flux are also considered. Our results are reduced to the known solutions in the existing literature for viscous fluid. Finally, we have plotted some graphical illustration to see the physical insight of the studied problem for different flow parameters and found that fluid velocity can be enhanced with the Caputo-Fabrizo approach by increasing the value of non-integer order parameter while skin friction coefficient decreases.

Introduction

The boundary layer flow and the heat and mass transfer on a surface is stretched over an conventional spectacular concentration due to their wide applications in industry, engineering, and metallurgy process. The transfer of heat is important because the rate of cooling can be restricted and final products of desired characteristics might be achieved. The flow on a flat plate with regular free stream has been examined by Basius [1].

The study of non-Newtonian fluids has established great attention in modern technologies such as geothermal engineering, geophysical, astrophysical bio-fluid and petroleum industries. Several basic relations of non- Newtonian fluids have been considered in the literature due to its resourceful nature. Non-Newtonian fluids have gotten the thought of specialist due to their modern and designing applications, i.e. passing on of paper, plastics production, material industry, nourishment handling, wire and edge covering and development of organic liquids. Experimentally, it has been observed that blood can be treated as non-Newtonian fluid at low shear rates in small arteries. Many physiological systems are modeled for biological tissues as porous layers. There are several proposed non-Newtonian fluid models to describe the behavior of these bio fluids. Among them Jeffrey fluid is the generalization of Newtonian fluid. In the existing literature, several scientists have studied Jeffrey fluid under different mechanical and thermal boundary conditions [2–8].

Now, metallurgical procedures, such as drawing and retreating of copper wires which involve cooling strips of continuous filaments, the MHD effect is to improve the rate of cooling. Mansur and Ishak [9] studied the MHD boundary layer flow of a nano fluid numerically. Ahmed et al. [10] applied the linearization method to the study of radiation effects on MHD boundary layer convective heat transfer in a porous media with low pressure gradient. A number of researchers discussed the MHD effects on Jeffrey fluid. Hayat et al. [11] found the chain solutions of MHD Jeffrey fluid in a channel. Das et al. [12] discussed Jeffrey fluid with MHD and slip condition. Jena et al. [13] found heat generation effects on MHD Jeffery fluid through a porous medium. Imtiaz et al. [14] found the effects of heterogeneous and homogenous reactions on MHD Jeffrey fluid. Ahmad and Ishak [15] studied the effects of viscous dissipation effects on a Jeffrey fluid with MHD. Different studies on MHD flow on physical situations were considered for an example in Refs. [16–18].

Fractional calculus is the natural generalization of classical calculus because it involves the derivatives and integral of non-integer order. The concept of fractional is odd but recently it attracts the scientists and

* Corresponding author.
E-mail address: ilyaskhan@tdt.edu.vn (I. Khan).

https://doi.org/10.1016/j.rinp.2018.04.008
Received 6 February 2018; Received in revised form 3 April 2018; Accepted 5 April 2018
Available online 12 April 2018
2211-3797/ © 2018 The Authors. Published by Elsevier B.V. This is an open access article under the CC BY-NC-ND license (http://creativecommons.org/licenses/BY-NC-ND/4.0/).

Nomenclature

u	Velocity of the fluid [ms^{-1}]
C	Concentration of the fluid [$kg\,m^{-3}$]
Gm	Thermal Grashof number [—]
C_w	Concentration level at the plate [$kg\,m^{-3}$]
C_p	Specific heat at a constant pressure [$j\,kg^{-1}\,K^{-1}$]
T_∞	Fluid temperature far away from the plate [K]
T_w	Fluid temperature at the plate [K]
C_∞	Concentration of the fluid Far away from the plate [$kg\,m^{-3}$]
M	Magnetic parameter

Greek symbols

α	Fractional parameter
ν	Kinematic viscosity of the fluid [$m^2\,s^{-1}$]
λ	Jeffery fluid parameter
β_T	Volumetric coefficient of mass expansion [K^{-1}]
β_C	Volumetric coefficient of thermal expansion [$m^3\,kg^{-1}$]
g	Acceleration due to gravity [$m\,s^{-2}$]
Gr	Thermal Grashof number [—]
k	Fluid thermal conductivity [$Wm^{-2}\,K^{-1}$]
D	Mass diffusivity [$m^2\,s^{-1}$]
Pr	Prandtl number [$=\mu c_p/k$]
Sc	Schmidt number [$=\nu/D$]
T	Temperature of the fluid [K]
s	Laplace transform parameter
t	Time [s]
μ	Dynamic viscosity [$kg\,m^{-1}\,s^{-1}$]
ρ	Fluid density [$kg\,m\,s^{-3}$]
λ_1	Ratio of relaxation and retardation time
λ_2	Retardation time [s]
λ_3	$\frac{Gm}{Gr}$ [——]

researchers and proved to be a powerful and widely used for controlling many physical process in different areas of engineering and science [19–23]. Being non-local operators they are defined using integrals. Therefore, the fractional derivative in time contains information about the function at earlier points, thus it possesses a memory effect. More exactly, such derivatives consider the history and non-local distribution effects which are necessary for better description and understanding of complex behavior. In (2015) Caputo-Fabrizio introduced new definition of fractional derivative without singular kernel [24]. After that researchers have applied this technique to many practical problems for instance [25–34].

In (2017) Aziz [35] studied the heat and mass transfer of unsteady hydromagnetic free convection flow through porous medium past a vertical plate with uniform surface heat flux for Newtonian fluid without fractional derivative. In the best of our knowledge there is no study has been carried out the fractional model of [35] with Caputo-Fabrizio fractional derivative. Therefore, we have extended the problem to some non-Newtonian fluid namely Jeffrey's fluid with Caputo-Fabrizio fractional derivative in the absence of porous media using numerical inverse Laplace transform technique.

Mathematical formulation of the problem

Consider electrical conducting incompressible generalized Jeffrey's fluid over an infinite vertical plate taken along x -axis in a porous medium and y -axis is perpendicular on the plate. At the beginning, the fluid and the plate have same temperature and concentration. After time $t > 0$, the plate starts to move with uniform acceleration At in x -direction against the gravitational acceleration. At the same time, heat from plate to the fluid is maintained throughout the flow at uniform rate and concentration raised to the constant level as shown in geometry of the problem. Further assume that magnetic Reynolds number is very small and Soret and thermal buoyancy effects are also considered. As the plate is of infinite length so all the physical variables become the functions of $y-$ space and time variable. Under the above mentioned assumptions and Boussinesq's approximation, set of equations for unsteady Jeffrey fluid [34,35] are as follows:

$$\frac{\partial u^*}{\partial t^*} = \frac{\nu}{1+\lambda_1}\left(1+\lambda_2\frac{\partial}{\partial t^*}\right)\frac{\partial^2 u^*}{\partial^2 y^*} - \frac{\sigma B_0^2}{\rho}u^* + g\beta_T(T^*-T_\infty^*) + g\beta_C(C^*-C_\infty^*), \tag{1}$$

$$\rho c_p\frac{\partial T^*}{\partial t^*} = k\frac{\partial^2 T^*}{\partial y^{*2}} + \frac{16\sigma T_\infty^3}{3k_1}\frac{\partial^2 T^*}{\partial y^{*2}} - Q_1(T^*-T_\infty^*) \tag{2}$$

$$\frac{\partial C^*}{\partial t^*} = D\frac{\partial^2 C^*}{\partial y^{*2}} + \frac{DK_T}{T_m}\frac{\partial^2 T^*}{\partial y^{*2}} - K_r^*(C^*-C_\infty^*), \tag{3}$$

Associated initial and boundary conditions:

$$t^* \leqslant 0: \; u^* = 0, \quad T^* = T_\infty^*, \quad C^* = C_\infty^*, \; \forall \; y^* \geqslant 0, \tag{4}$$

$$t^* > 0: \; u^* = At^*, \quad \frac{\partial T^*}{\partial y^*} = -\frac{q_w''}{k}, \quad C^* = C_w^*, \; at \quad y^* = 0, \tag{5}$$

$$t^* > 0: \; u^* \to 0, \quad T^* \to T_\infty^*, \quad C^* \to C_\infty^* \; \; as\, y^* \to \infty, \tag{6}$$

in which A is the uniform acceleration of the plate, x^* and y^* are the distances along and perpendicular to the plate, t^* is the dimensional time, u^* is the fluid velocity in the x^* -direction, T^* is the temperature of the fluid, T_∞^* is the free stream temperature, C^* is the concentration, C_w^* is the surface concentration, C_∞^* is the free stream concentration, Q_1 is the dimensional heat absorption coefficient, k is the thermal conductivity, q_w'' is the constant heat flux per unit area at the plate, β_T is the volumetric coefficient of thermal expansion, β_C is the volumetric coefficient of expansion for concentration, ν is the kinematic viscosity, μ is the fluid viscosity, ρ is the fluid density, c_p is the specific heat capacity, σ is the electrical conductivity of the fluid, T_m is the mean fluid temperature, K_T is the thermal-diffusion ratio, K_r^* is the chemical reaction constant and D is the mass diffusivity. Now, we define the following non-dimensional variables

$$u = \frac{u^*}{(\upsilon A)^{\frac{1}{3}}}, \quad y = \frac{y^* A^{\frac{1}{3}}}{\upsilon^{\frac{2}{3}}}, \quad t = \frac{t^* A^{\frac{2}{3}}}{\upsilon^{\frac{1}{3}}}, \quad T = \frac{T^*-T_\infty^*}{\left(\frac{q_w''}{k}\right)}\frac{A^{\frac{1}{3}}}{\upsilon^{\frac{2}{3}}}, \quad C = \frac{C^*-C_\infty^*}{C_w^*-C_\infty^*}. \tag{7}$$

Putting Eq. (7) in Eqs. (1)(6) and in the resulting momentum equation using the substitution $u(y,t) = GrU(y,\tilde{t})$ and then replacing integer order time derivative with non-integer order derivative of order α.

$$D_t^\alpha U(y,\tilde{t}) = \frac{1}{1+\lambda_1}(1+\lambda D_t^\alpha)\frac{\partial^2 U(y,\tilde{t})}{\partial y^2} - MU(y,\tilde{t}) + T(y,\tilde{t}) + \lambda_3 C(y,\tilde{t}), \tag{8}$$

$$D_t^\alpha T(y,\tilde{t}) = \frac{1+R}{\mathrm{Pr}}\frac{\partial^2 T(y,\tilde{t})}{\partial y^2} - Q_H T(y,\tilde{t}), \tag{9}$$

$$D_t^{\alpha} C(y,\tilde{t}) = \frac{1}{Sc}\frac{\partial^2 C(y,\tilde{t})}{\partial y^2} + S_r \frac{\partial^2 T(y,\tilde{t})}{\partial y^2} - \gamma C(y,\tilde{t}). \tag{10}$$

The Caputo-Fabrizio time fractional derivative of order $\alpha \in [0,1]$ is defined as [24]

$${}^{CF}D_t^{\alpha} f(y,t) = \frac{1}{(1-\alpha)}\int_0^t \exp\left(-\frac{\alpha(t-\tau)}{1-\alpha}\right)\frac{\partial f(y,\tau)}{\partial \tau}d\tau. \tag{11}$$

The Laplace transform of Caputo-Fabrizio time derivative is

$$L\{{}^{CF}D_t^{\alpha} f(y,t)\} = \frac{sL\{f(y,t)\} - f(y,0)}{(1-\alpha)s + \alpha}. \tag{12}$$

with dimensionless initial and boundary conditions

$$\begin{cases} \tilde{t} \leqslant 0:\ U(y,\tilde{t}) = 0, T(y,\tilde{t}) = 0,\ \ C(y,\tilde{t}) = 0,\ y \geqslant 0, \\ \tilde{t} > 0:\ U(y,\tilde{t}) = \tilde{t}, \frac{\partial T(y,\tilde{t})}{\partial y} = -1, C(y,\tilde{t}) = 1, at\ y = 0, \\ \tilde{t} > 0:\ U(y,\tilde{t}) \to 0, T(y,\tilde{t}) \to 0, C(y,\tilde{t}) \to 0, as y \to \infty, \end{cases} \tag{13}$$

where

$$\begin{cases} M = \frac{\sigma B_0^2 \sqrt[3]{\upsilon A}}{\rho A},\ \gamma = K_r' \sqrt[3]{\frac{\upsilon}{A^2}}, & Gm = \frac{g\beta'(C_w' - C_{\infty}')}{A},\ \lambda = \lambda_2 \sqrt[3]{\frac{A^2}{\gamma}} \\ \frac{1}{K} = \frac{\upsilon \sqrt[3]{\upsilon A}}{AK'},\ Gr = \frac{g\beta q_w' \sqrt[3]{\frac{\upsilon^2}{A}}}{Ak}, & Pr = \frac{\upsilon \rho c_p}{k},\quad \tilde{t} = \frac{t}{Gr},\quad \lambda_3 = \frac{Gm}{Gr} \\ Q_H = \frac{Q_1}{\rho c_p \sqrt[3]{\frac{A^2}{\upsilon}}},\ Sc = \frac{\upsilon}{D}, & Sr = \frac{DK_T q_w' \sqrt[3]{\frac{1}{\upsilon A}}}{T_m k (C_w' - C_{\infty}')},\quad F = \frac{\Pr}{1+R}. \end{cases} \tag{14}$$

Temperature filed

By applying Laplace transform to Eq. (9) keeping in mind the initial condition

$$\frac{\partial^2 \overline{T}}{\partial y^2} = \left(\frac{F\tilde{s}}{\tilde{s}(1-\alpha) + \alpha} + FQ_H\right)\overline{T}, \tag{15}$$

satisfy the conditions

$$\frac{\partial \overline{T}}{\partial y} = -\frac{1}{\tilde{s}},\ \overline{T} \to 0, as\ y \to \infty. \tag{16}$$

Solution of Eq. (15) subject to conditions Eq. (16)

$$\begin{aligned} \overline{T}(y,\tilde{s}) &= \frac{1}{\sqrt{F(a_o + Q_H)}}\frac{1}{\sqrt{\frac{\tilde{s}+\beta_1}{\tilde{s}+a_1}}}\frac{1}{s}\exp\left(-y\sqrt{F(a_o+Q_H)\frac{\tilde{s}+\beta_1}{\tilde{s}+a_1}}\right), \overline{T}(y,\tilde{s}) \\ &= \frac{1}{\sqrt{F(a_o+Q_H)}}\psi_1(0,\tilde{s},a_1,\beta_1)\psi_2(y,\tilde{s},a_1,\beta_1), \end{aligned} \tag{17}$$

Inverse Laplace transform of the Eq. (17) using convolution theorem.

$$T(y,\tilde{t}) = \frac{1}{\sqrt{F(a_o+Q_H)}}\int_0^t \psi_1(0,(\tilde{t}-\tau),a_1,\beta_1)\psi_2(y,\tau,a_1,\beta_1)d\tau. \tag{18}$$

For the ordinary case when, result is identical to those obtained by Aziz [35] and presented graphically in Fig. 12 for the validation of our obtained result.

Concentration field

By applying Laplace transform of Eq. (10) by using the initial condition

$$\frac{1}{Sc}\frac{\partial^2 \overline{C}}{\partial y^2} - \left(\gamma + \frac{\tilde{s}}{\tilde{s}(1-\alpha)+\alpha}\right)\overline{C} = -Sr\frac{\partial^2 \overline{T}}{\partial y^2}, \tag{19}$$

satisfy the conditions

$$\overline{C} = \frac{1}{\tilde{s}},\ \overline{C} \to 0, as\ y \to \infty. \tag{20}$$

Solution of Eq. (19) subject to conditions (20), we have

$$\begin{aligned} \overline{C}(y,\tilde{s}) = {} & \frac{1}{\tilde{s}}\exp\left(-y\sqrt{Sc(a_o+\gamma)\frac{\tilde{s}+\beta_2}{\tilde{s}+a_1}}\right) \\ & + \frac{ScSr\sqrt{(\tilde{s}+a_1)}\sqrt{(\tilde{s}+\beta_1)}}{\sqrt{F(a_o+Q_H)}[(1-Sc)s + (\beta_1 - \beta_2 Sc_1]} \\ & \left[\frac{\exp\left(-y\sqrt{Sc(a_o+\gamma)\frac{\tilde{s}+\beta_2}{\tilde{s}+a_1}}\right)}{s}\right. \\ & \left. -\frac{\exp\left(-y\sqrt{F(a_o+Q_H)\frac{\tilde{s}+\beta_1}{\tilde{s}+a_1}}\right)}{s}\right]\overline{C}(y,\tilde{s}) = \psi_3(y,\tilde{s},a_1,\beta_2) \\ & + \frac{ScSr}{\sqrt{F(a_o+Q_H)}}\psi_4(0,\tilde{s},a_1,\beta_1,\beta_2)[\psi_3(y,\tilde{s},a_1,\beta_2) - \psi_2(y,\tilde{s},a_1,\beta_1)]. \end{aligned} \tag{21}$$

with its inverse Laplace transform of Eq. (21) and using convolution theorem,

$$\begin{aligned} C(y,\tilde{t}) = {} & \psi_3(y,\tilde{t},a_1,\beta_2) + \frac{ScSr}{\sqrt{F(a_o+Q_H)}}\int_0^t \psi_4(0,\tilde{t} \\ & -\tau,a_1,\beta_1,\beta_2)[\psi_3(y,\tau,a_1,\beta_2) - \psi_2(y,\tau,a_1,\beta_1)]d\tau. \end{aligned} \tag{22}$$

For the ordinary case when $\alpha \to 1$, result is identical to those obtained by Aziz [35] and presented graphically in Fig. 12 for the validation of our obtained result.

Velocity field

By applying Laplace transform of Eq. (8) by using the initial condition

$$\begin{aligned} & \frac{1}{1+\lambda_1}\left(1 + \frac{\lambda a_0 \tilde{s}}{\tilde{s}+a_1}\right)\frac{\partial^2 \overline{U}(y,\tilde{s})}{\partial y^2} - \left(M + \frac{a_0\tilde{s}}{\tilde{s}+a_1}\right)\overline{U}(y,\tilde{s}) \\ & = -\overline{T}(y,\tilde{s}) - \lambda_3 \overline{C}(y,\tilde{s}). \end{aligned} \tag{23}$$

Introducing the expressions of temperature and concentration from Eqs. (17) and (21) in Eq. (23)

$$\begin{aligned} & \frac{1}{1+\lambda_1}\left(1 + \frac{\lambda a_0 \tilde{s}}{\tilde{s}+a_1}\right)\frac{\partial^2 \overline{U}(y,\tilde{s})}{\partial y^2} - \left(M + \frac{a_0\tilde{s}}{\tilde{s}+a_1}\right)\overline{U}(y,\tilde{s}) \\ & = -\frac{1}{\tilde{s}}\frac{1}{\sqrt{F(a_o+Q_H)}}\sqrt{\frac{\tilde{s}+\beta_1}{\tilde{s}+a_1}}\exp\left(-y\sqrt{F(a_o+Q_H)\frac{\tilde{s}+\beta_1}{\tilde{s}+a_1}}\right) \\ & -\lambda_3\frac{\exp\left(-y\sqrt{Sc(a_o+\gamma)\frac{\tilde{s}+\beta_2}{\tilde{s}+a_1}}\right)}{s} \\ & -\frac{\lambda_3 ScSr\sqrt{(\tilde{s}+a_1)}\sqrt{(\tilde{s}+\beta_1)}}{\sqrt{F(a_o+Q_H)}[(1-Sc)\tilde{s} + (\beta_1 - \beta_2 Sc_1]} \\ & \times\times[\frac{\exp\left(-y\sqrt{Sc(a_o+\gamma)\frac{\tilde{s}+\beta_2}{\tilde{s}+a_1}}\right)}{\tilde{s}} - \frac{\exp\left(-y\sqrt{F(a_o+Q_H)\frac{\tilde{s}+\beta_1}{\tilde{s}+a_1}}\right)}{\tilde{s}}], \end{aligned} \tag{24}$$

satisfy the conditions

$$\overline{U} = \frac{1}{\widetilde{s}^2},\ \overline{U} \to 0,\ as\ y \to \infty. \tag{25}$$

Solution of Eq. (24) subject to conditions (25)

$$\begin{aligned}\overline{U}(y,\widetilde{s}) &= \frac{1}{\widetilde{s}^2}\exp\left(-y\sqrt{\frac{(1+\lambda_1)(M+a_0)}{1+\lambda a_0}}\sqrt{\widetilde{s}+\beta_4}\right)\\ &+ \frac{(1+\lambda_1)(\widetilde{s}+a_1)^2\sqrt{\widetilde{s}+a_1}\left[\exp\left(-y\sqrt{\frac{(1+\lambda_1)(M+a_0)}{1+\lambda a_0}}\sqrt{\widetilde{s}+\beta_4}\right)-\exp\left(-y\sqrt{F(Q_H+a_0)}\sqrt{\widetilde{s}+\beta_1}\right)\right]}{\sqrt{F(Q_H+a_0)}[(1+\lambda a_0)(FQ_H+Fa_0)(\widetilde{s}+\beta_1)(\widetilde{s}+\beta_3)-(1+\lambda_1)(M+a_0)(\widetilde{s}+a_1)(\widetilde{s}+\beta_4)]\sqrt{\widetilde{s}+\beta_1}\widetilde{s}}\\ &+ \frac{\lambda_3 ScSr(1+\lambda_1)(\widetilde{s}+a_1)^2\sqrt{\widetilde{s}+a_1}\sqrt{\widetilde{s}+\beta_1}\times\left[\exp\left(-y\sqrt{\frac{(1+\lambda_1)(M+a_0)}{1+\lambda a_0}}\sqrt{\widetilde{s}+\beta_4}\right)\right.}{\left.-\exp\left(-y\sqrt{Sc(\gamma+a_0)}\sqrt{\frac{\widetilde{s}+\beta_2}{\widetilde{s}\frac{\delta y}{\delta x}+a_1}}\right)\right]}\\ &+ \frac{}{\sqrt{F(Q_H+a_0)}(1-Sc)[(1+\lambda a_0)(Sc\gamma+Sca_0)(\widetilde{s}+\beta_2)(\widetilde{s}+\beta_3)-(1+\lambda_1)(M+a_0)(\widetilde{s}+a_1)(\widetilde{s}+\beta_4)](\widetilde{s}+Sc_2)\widetilde{s}}\\ &- \frac{\lambda_3 ScSr(1+\lambda_1)(\widetilde{s}+a_1)^2\sqrt{\widetilde{s}+a_1}\sqrt{\widetilde{s}+\beta_1}\times\left[\exp\left(-y\sqrt{\frac{(1+\lambda_1)(M+a_0)}{1+\lambda a_0}}\sqrt{\widetilde{s}+\beta_4}\right)\right.}{\left.-\exp\left(-y\sqrt{F(Q_H+a_0)}\sqrt{\widetilde{s}+\beta_1}\right)\right]}\\ &- \frac{}{\sqrt{F(Q_H+a_0)}(1-Sc)[(1+\lambda a_0)(FQ_H+Fa_0)(\widetilde{s}+\beta_2)(\widetilde{s}+\beta_3)-(1+\lambda_1)(M+a_0)(\widetilde{s}+a_1)(\widetilde{s}+\beta_4)](\widetilde{s}+Sc_2)\widetilde{s}}\\ &+ \frac{(1+\lambda_1)(\widetilde{s}+a_1)^2\left[\exp\left(-y\sqrt{\frac{(1+\lambda_1)(M+a_0)}{1+\lambda a_0}}\sqrt{\widetilde{s}+\beta_4}\right)-\exp\left(-y\sqrt{Sc(\gamma+a_0)}\sqrt{\widetilde{s}+\beta_2}\right)\right]}{[(1+\lambda a_0)(Sc\gamma+Sca_0)(\widetilde{s}+\beta_2)(\widetilde{s}+\beta_3)-(1+\lambda_1)(M+a_0)(\widetilde{s}+a_1)(\widetilde{s}+\beta_4)]\widetilde{s}}\end{aligned} \tag{26}$$

where

$$a_0 = \frac{1}{1-\alpha},\quad a_1 = \frac{\alpha}{1-\alpha},\quad \beta_1 = \frac{Q_H a_1}{Q_H + a_0},\quad \beta_2 = \frac{\gamma a_1}{\gamma + a_0},\quad \beta_3 = \frac{a_1}{1+\lambda a_0},\quad \beta_4 = \frac{Ma_1}{M+a_0},\quad Sc_1 = \frac{Sc(\gamma+a_0)}{(Q_H+a_0)},\quad Sc_2 = \frac{\beta_1-\beta_2 Sc_1}{1-Sc_1}.$$

In complex transform domains we can't find inverse Laplace transform analytically for some practical applications. So, we have used some numerical techniques to obtained inverse Laplace transform of Eq. (26). By using Stehfest's algorithm [36] and Tzou's [37] for numerical Laplace method in solving the fractional differential equations.

Results and discussion

Exact analysis of non-Newtonian fluid has been discussed with the help of Laplace transform method. Now, we have computed the results for a variety of physical parameters which are represented in the graphs. The results which we obtained to illustrate the effects of magnetic field parameter M, λ_3 ration between mass and heat transfer Grashof numbers, chemical reaction parameter γ, Prandtl number Pr, heat absorption parameter Q_H, radiation parameter R, Schmidt number Sc, Soret number Sr and dimensionless time t on velocity profile only.

The variation of velocity profile with different values of magnetic parameter M is shown in Fig. 1. MHD principal used as an agent to control the boundary layer thickness. As expected, by increasing value of M, reduces the fluid velocity remarkably. Further, it can be seen that the boundary layer thickness and decreasing in the main free stream region. This happened physically due to the reason that drag force acting opposite to the fluid flow and reduced the fluid velocity. The buoyancy ratio parameter λ_3 represents the ratio between mass and thermal buoyancy forces. When $\lambda_3 = 0$ there is no mass transfer and the buoyancy force is due to the thermal diffusion only. For $\lambda_3 > 0$ means that mass buoyancy force acts in the same direction of thermal buoyancy force. The influence λ_3 on velocity profile is shown in Fig. 2. It is

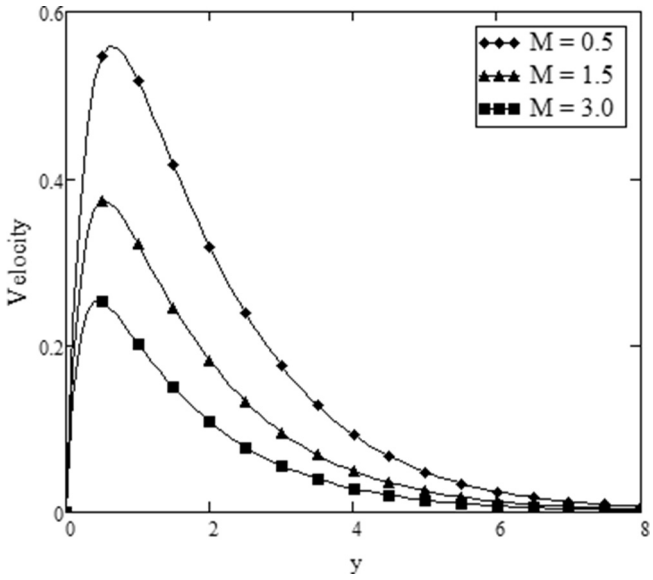

Fig. 1. Velocity profile for different values of M when $t = 2, R = 0.1, \mathrm{Pr} = 0.3, Q_H = 1, \gamma = 0.5, \lambda_3 = 1, Sr = 1, Sc = 0.22, \lambda = 0.1, \lambda_1 = 0.9, \alpha = 0.3$.

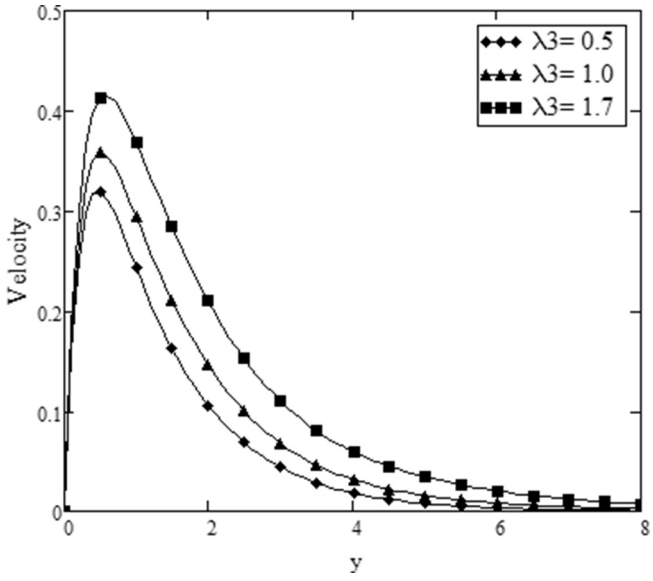

Fig. 2. Velocity profile for different values of λ_3 when $t = 2, R = 0.3, \mathrm{Pr} = 0.0.71, Q_H = 1, \gamma = 0.5$,

observed from figure that the increasing value of λ_3 which increases the velocity profile. It occurs due to the increase in buoyancy force which results to increase in the fluid velocity and increases the thickness of boundary layer. Clearly the velocity is maximum for larger value of λ_3 near the plate and for larger y decreases in the free stream region and then approaches to zero. Fig. 3 presents the increasing values of the chemical reaction parameter γ on the velocity profiles. It can see that the increasing values of γ leads to fall in the fluid velocity field. Physically, the positive chemical reactions are treated as destructive and negative chemical reactions termed as generative or constructive chemical reactions. That's why the fluid velocity reduced due to increase in the value of positive chemical reaction parameter. Fig. 4 shows the

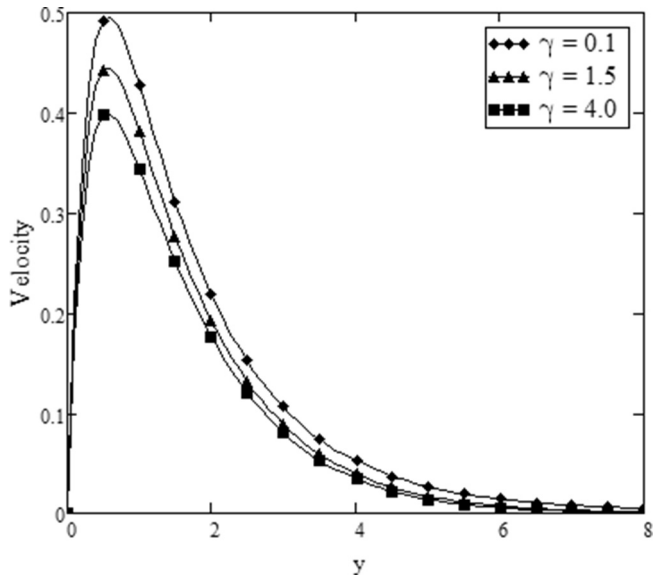

Fig. 3. V. elocity profile for different values of γ when $t = 2, R = 0.1, \Pr = 0.1, Q_H = 10, M = 0.2,$ $\lambda_3 = 1, Sr = 1, Sc = 0.22, \lambda = 0.1, \lambda_1 = 0.9, \alpha = 0.3.$

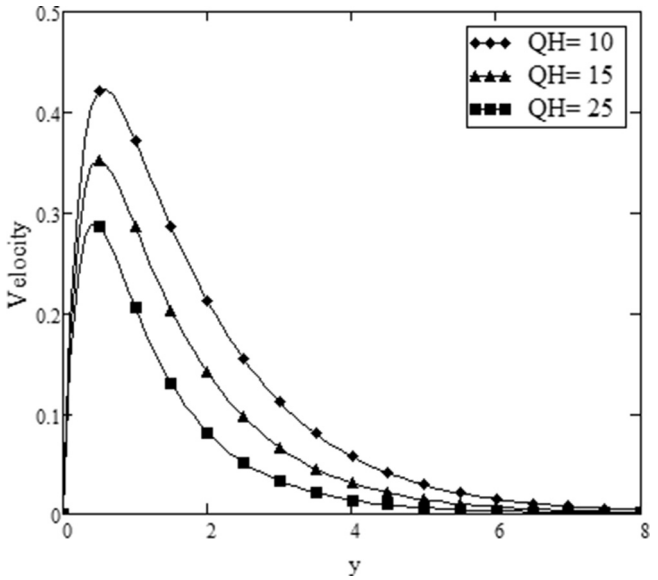

Fig. 5. Velocity profile for different values of Q_H when $t = 2, R = 1, \gamma = 0.5, \Pr = 0.1, M = 1,$ $\lambda_3 = 1, Sr = 1, Sc = 0.22, \lambda = 0.1, \lambda_1 = 0.9, \alpha = 0.3.$

effect of Pr on velocity profiles. It is observed that the increasing value of Prandtl number Pr results in decrease the velocity profile. This is because of the fact that higher viscosity of fluid with the large amount of Pr and a small thermal conductivity, which disturb the fluid velocity and makes a fluid thick. Fig. 5 presents the velocity disturbance along the boundary layer by the influence of heat absorption parameter Q_H. It is observed from the figure that the increasing values of Q_H which decreases the distributions of the fluid velocity. This is because of the presence of heat in the layers of boundary absorb some amount of energy and due to this fact decreases the temperature of fluid and hence fluid velocity. Fig. 6 shows the influence of radiation parameter R on the velocity profiles. It is observed from the figure that the increasing value of R also increases the velocity profile. This is due to the fact that the large values of R which increases the control of conduction over radiation by increasing the buoyancy force and finally increased the fluid velocity. The effect of Schmidt number Sc on the velocity profiles are shown in Fig. 7. It is observed that the increasing value of Schmidt number which decreases the velocity profile due to the decrease in the molecular diffusivity, which also decreases the concentration and thickness along the boundary layers. Fig. 8 presents the effect of Soret number Sr on the velocity profiles. It is observed that increasing value of Soret number Sr increases the velocity profile due to the increase in the molecular diffusivity. Fig. 9 shows the variation of different values for time t with the velocity profiles. It is observed that the increasing

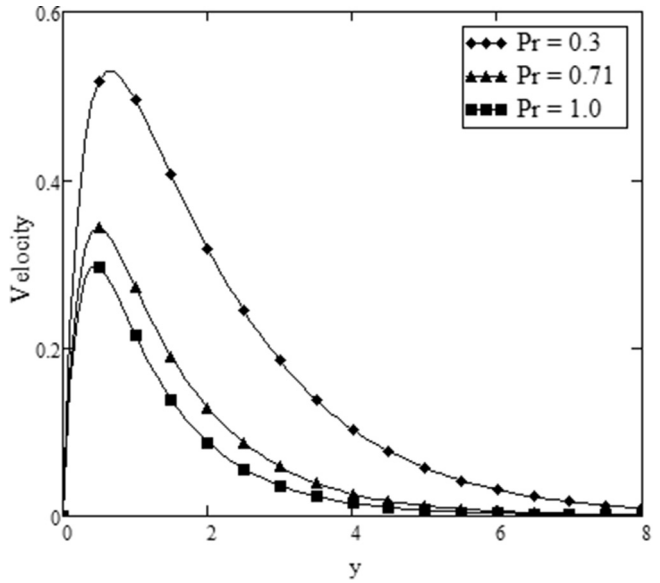

Fig. 4. Velocity profile for different values of Pr when $t = 2, R = 0.1, \gamma = 0.5, Q_H = 0.5, M = 1,$ $\lambda_3 = 1, Sr = 1, Sc = 0.22, \lambda = 0.1, \lambda_1 = 0.9, \alpha = 0.3.$

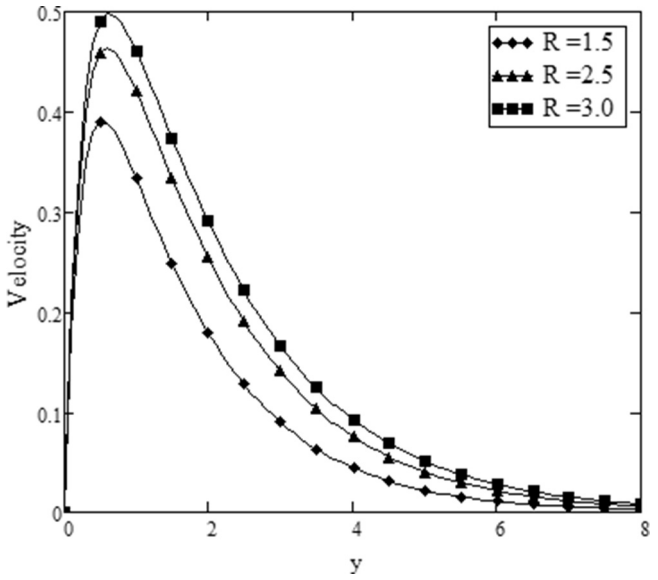

Fig. 6. Velocity profile for different values of R when $t = 2, Q_H = 15, \gamma = 0.5, \Pr = 0.1, M = 1,$ $\lambda_3 = 1, Sr = 1, Sc = 0.22, \lambda = 0.1, \lambda_1 = 0.9, \alpha = 0.3.$

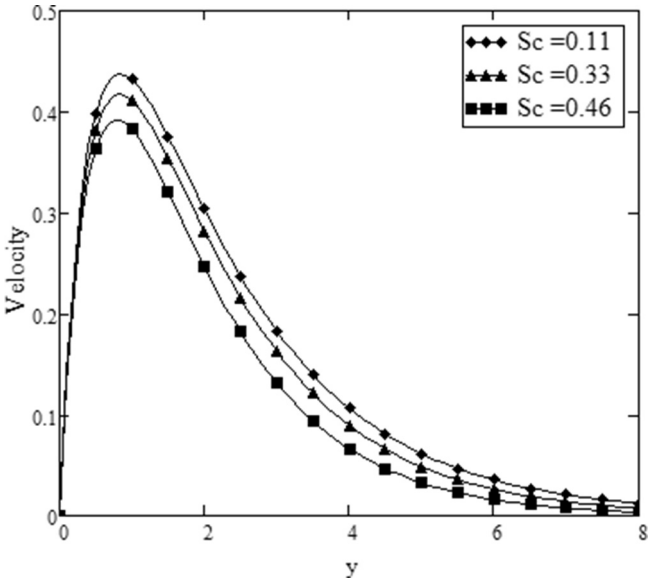

Fig. 7. Velocity profile for different values of Sc when $t = 2, Q_H = 0.1, \gamma = 0.5, \mathrm{Pr} = 0.31, R = 0.1, \lambda_3 = 1, Sr = 1, M = 1, \lambda = 0.1, \lambda_1 = 0.9, \alpha = 0.3$.

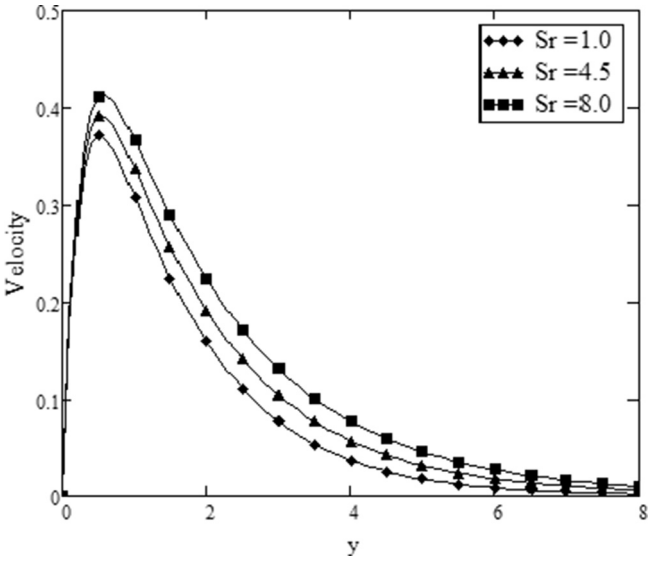

Fig. 8. Velocity profile for different values of Sr when $t = 2, Q_H = 7, \gamma = 0.5, \mathrm{Pr} = 0.1, R = 0.1,$

values of time t which increase the rate of velocity too. Furthermore, the velocity takes the values of time t at the plate ($y = 0$) and tends to 0 for the larger values of y that justifies the natural boundary condition. Fig. 10 shows the variation of velocity profile against y for the variation of α by fixing other flow parameters. It is observed that the increasing values of α increases the velocity. Physically, using the time fractional derivative of non-singular kernel fluid velocity can be enhanced. Fig. 11 represents the variation of parameter λ against the velocity profile and found that fluid velocity is an increasing function of parameter λ. Figs. 12–14 are plotted for the validation of our obtained results for temperature, concentration and velocity fields and observed that they

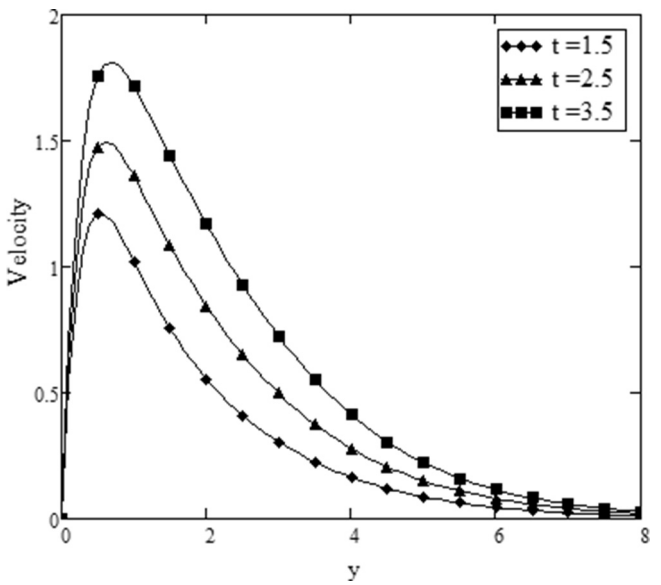

Fig. 9. Velocity profile for different values of t when $Q_H = 0.2, \gamma = 0.5, \mathrm{Pr} = 0.71, R = 0.1, M = 1, \lambda_3 = 1, Sc = 0.22, Sr = 1, \lambda = 0.1, \lambda_1 = 0.9, \alpha = 0.3$.

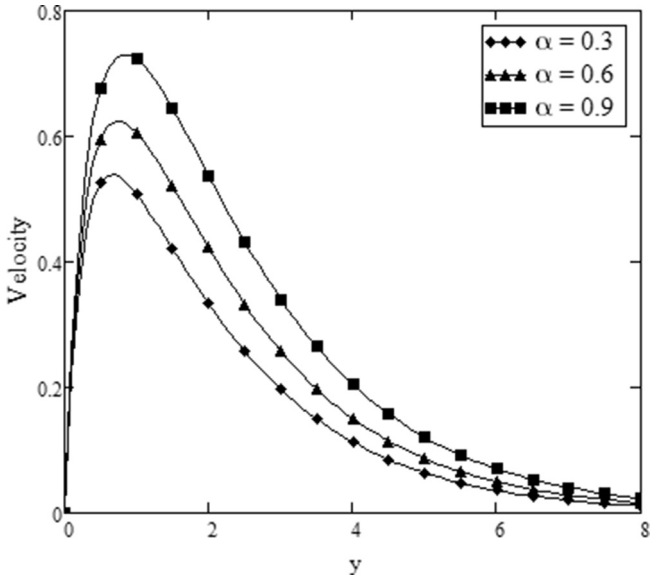

Fig. 10. Velocity profile for different values of α when $t = 2, Q_H = 3, \gamma = 0.5, \mathrm{Pr} = 0.1, R = 0.1, \lambda_3 = 1, M = 1, Sc = 0.22, Sr = 1, \lambda = 0.1, \lambda_1 = 0.9$.

are in good agreement with [35] when the fractional parameter $\alpha \to 1$ for temperature and concentration respectively. Since we have solved the problem of non-Newtonian fluid for velocity field and taking $\alpha \to 1, \lambda \to 0, \lambda_1 \to 0$ in the obtained solution we recovered the results obtained by those [35] with $\frac{1}{K} = 0$ and presented in Fig. 14. For numerical Laplace transform of temperature, concentration and velocity fields table 1 is presented. Table 2 explains the influence of fractional parameter on skin friction and found that skin friction remarkably reduced by increasing the values of fractional parameter α.

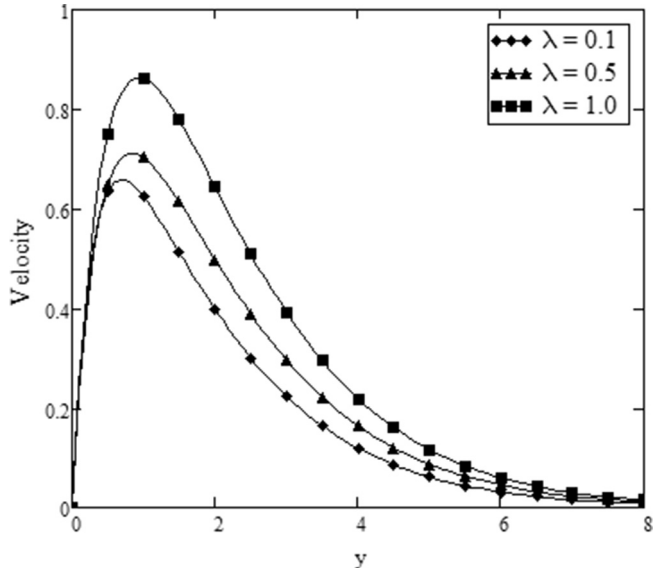

Fig. 11. Velocity profile for different values of λ when $t = 2, Q_H = 1, \gamma = 0.5, \Pr = 0.3, R = 0.1$.

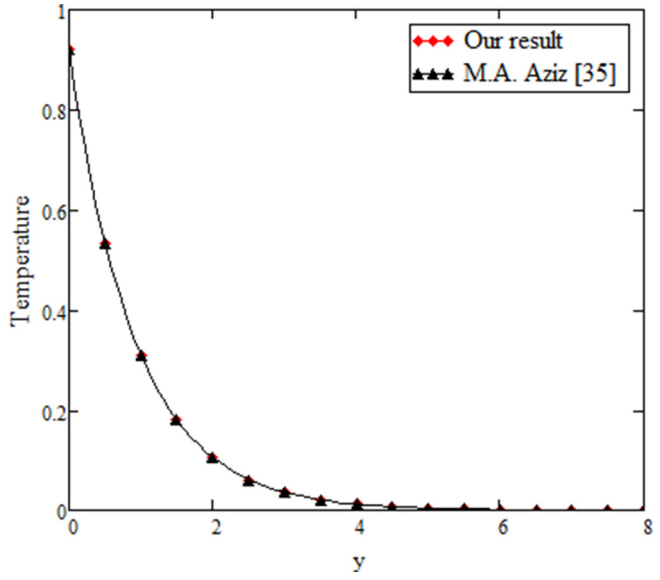

Fig. 12. Temperature profile for comparison of our result when $\alpha \to 1$, $Q_H = 13$, $\Pr = 0.1$, $R = 0.1$.

Conclusion

Finally, from the exact analysis of Jeffrey's fractional fluid some concluding remarks are given as

- Fluid velocity is a decreasing function of the following parameters $M, \gamma, \Pr, Q_H, Sc$.
- By increasing the values of $\lambda_3 R, Sr, t$ fluid velocity increases.
- By increasing the value of Jeffrey parameter λ and fractional parameter α fluid flow can also be enhanced.
- Skin friction decreases by increasing the value of fractional parameter.
- Our solutions for Jeffrey's fluid reduced to viscous fluid as a limiting case and they are in good agreement.

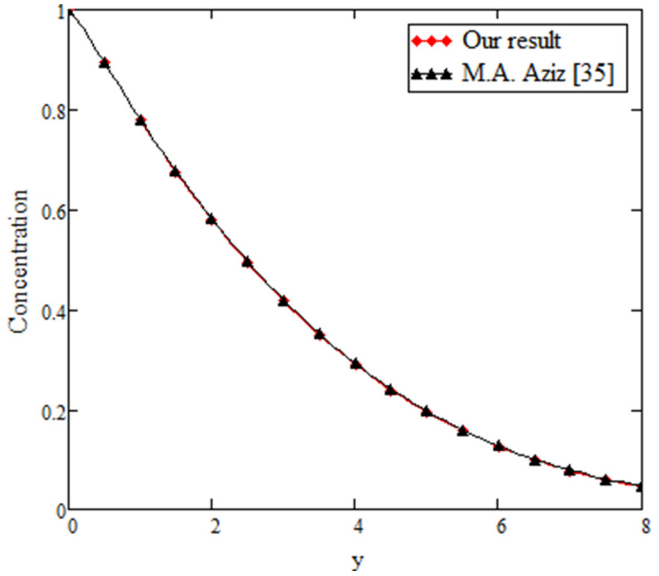

Fig. 13. Concentration profile for comparison of our result when $\alpha \to 1$, $Q_H = 5$, $\Pr = 7$, $R = 0.5$, $Sc = 0.22$, $Sr = 0.5$, $\gamma = 0.2$.

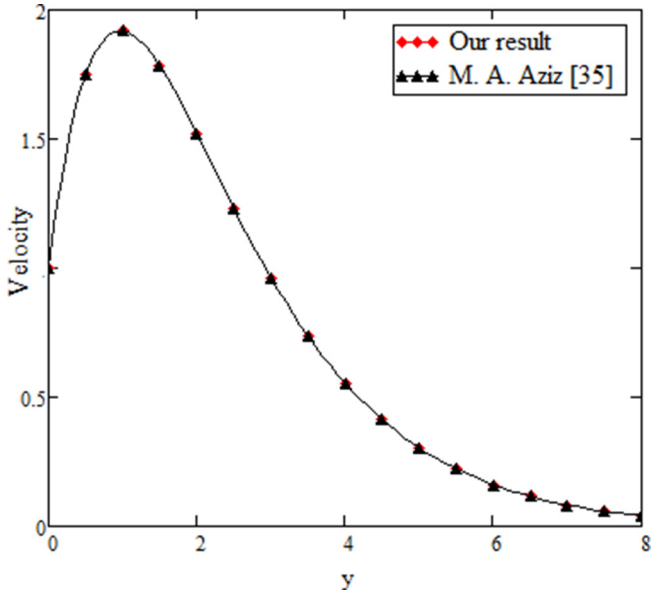

Fig. 14. Velocity profile for comparison of our result when $\lambda \to 0$, $\lambda_1 \to 0$, $\alpha \to 1$, $Q_H = 0.5$, $\Pr = 0.31$, $R = 2$, $Sr = 2$, $\lambda_3 = 2$, $M = 0.2$, $Sc = 0.22$, $\gamma = 0.5$, $\frac{1}{K} = 0$

Table 1
Inverse Laplace transform by Stehfest's and Tzou's formula.

y	$T(y,t)$ [Stehfest's]	$T(y,t)$ [Tzou's]	$C(y,t)$ [Stehfest's]	$C(y,t)$ [Tzou's]	$U(y,t)$[Stehfest's]	$U(y,t)$ [Tzou's]
1	0.505	0.505	0.279	0.279	0.173	0.173
2	0.283	0.283	0.155	0.155	0.117	0.117
3	0.159	0.159	0.006	0.006	0.067	0.067
4	0.089	0.089	0.047	0.047	0.037	0.037
5	0.05	0.05	0.026	0.026	0.02	0.02
6	0.028	0.028	0.014	0.014	0.011	0.011
7	0.016	0.016	7.269×10^{-3}	7.269×10^{-3}	6.109×10^{-3}	6.109×10^{-3}
8	8.801×10^{-3}	8.801×10^{-3}	3.781×10^{-3}	3.781×10^{-3}	3.336×10^{-3}	3.336×10^{-3}

Table 2
Effects of fractional parameter on Skin friction.

C_f $\alpha = 0$	C_f $\alpha = 0.2$	C_f $\alpha = 0.4$	C_f $\alpha = 0.6$	C_f $\alpha = 0.8$	C_f $\alpha = 0.99$
1.161	1.055	0.938	0.809	0.665	0.511
1.114	1.009	0.894	0.767	0.625	0.474
1.076	0.972	0.858	0.732	0.593	0.444
1.043	0.941	0.828	0.704	0.567	0.42
1.016	0.915	0.804	0.682	0.546	0.401
0.994	0.894	0.784	0.663	0.528	0.385
0.976	0.876	0.767	0.647	0.514	0.373
0.96	0.862	0.754	0.635	0.503	0.363
0.947	0.85	0.743	0.625	0.494	0.355
0.937	0.84	0.733	0.616	0.486	0.348
0.928	0.831	0.726	0.609	0.48	0.343
0.921	0.825	0.719	0.604	0.475	0.339
0.915	0.819	0.714	0.599	0.471	0.335
0.91	0.814	0.71	0.595	0.468	0.332
0.905	0.81	0.707	0.592	0.465	0.33
0.902	0.807	0.704	0.59	0.463	0.329

Acknowledgement

The authors are highly thankful to the reviewers for their fruitful suggestions to improve the manuscript and University of Management and Technology Pakistan for supporting and facilitating.

References

[1] H. Basius, Convective heat transfer, second Ed., Z Angew Math Phy, 56 (1908) 1–37.
[2] S. Dhananjaya, P.V. Arunachalam, S. Sreenadh, A. Parandhama, Free convection flow of a Jeffrey fluid between vertical plates partially filled with porous medium, Int J Sci Res Eng Technol (IJSRET), ISSN 2278 – 0882 4(5) (2015) 503–512.
[3] Sahoo B. Flow and heat transfer of a non-Newtonian fluid past a stretching sheet with partial slip. Commun Nonlinear Sci Numer Simul 2010;15:602–15.
[4] Tripathi D, Ali N, Hayat T, Chaube MK, Hendi AA. Peristaltic flow of MHD Jeffrey fluid through a finite length cylindrical tube. Appl Math Mech 2011;32:1148–60.
[5] Dalir N, Dehsara M, Nourazar SS. Entropy analysis for magnetohydrodynamic flow and heat transfer of a Jeffery nanofluid over a stretching sheet. Energy 2015;79:351–62.
[6] M. Pourabdian, M. Qate, M.R. Morad, A. Javare shkian, The Jeffery-Hamel flow and heat transfer of nanofluids by homotopy perturbation method and Comparison with Numerical Results, arXiv: 1601.05298 (2016).
[7] Zin NAM, Khan I, Shafie S. Influence of non-integer order parameter and Hartmann number on the heat and mass transfer flow of a Jeffery fluid over an oscillating vertical plate Caputo-Fabrizio time fractional derivatives. Math Prob Eng 2016.
[8] R. Ellahi, M.M. Bhatti, I. Pop, Effects of hall and ion slip on MHD peristaltic flow of Jeffrey fluid in a non-uniform rectangular duct, Int J Numer Methods Heat Fluid Flow 26 (2016) 1802.
[9] Mansur S, Ishak A. The megnetohydrodynamic boundary layer flow of a nanofluid past a stretching sheet with slip boundary conditions. J Appl Math 2016;9:1073–9.
[10] Ahmed MAM, Mohammad ME, Khidir AA. On linearization method to MHD boundary layer convective heat transfer with low pressure gradient. Prop Power Res 2015;4:105–23.
[11] Hayat T, Sajjad R, Asghar S. Series solution for MHD channel flow of Jeffery fluid. Commun Nonlinear Sci Numer Simul 2010;15:2400.
[12] Das K, Acharya N, Kundu PK. Thermal radiation in unsteady MHD free convection flow of Jeffery fluid. Alex Eng J 2015;54:815.
[13] S. Jena1, S.R. Mishra, G.C. Dash, Influence of non-integer order parameter and Hartmann number on the heat and mass transfer flow on Jeffery fluid over an oscillating vertical plate with Caputo-Fabrizio time fractional derivatives, Int J Appl Comp Math (2016).
[14] M. Imtiaz, T. Hayat, A. Alsaedi, PLoS ONE, MHD convection flow of Jeffery fluid due to a curved strechting surface with Homogenous Reactions (2016).
[15] Ahmad K, Ishak A. MHD flow and heat transfer of a Jeffery fluid over a stretching sheet with viscous dissipation. Malays J Math Sci 2016;10:311–23.
[16] Haiso KL. MHD mixed convection for viscolastic fluid past porous wedge. Int J Non-Linear Mech 2011;46:1–8.
[17] Haiso KL. Stagnation electrical MHD nanofluid mixed convection with slip boundary on a stretching sheet 2016;98:850–61.
[18] Shazad SA, Abbasi FM, Hayat T, Alsaedi F. Peristaltic in a curved channel with slip and radial magnetic field 2015;91:562–9.
[19] Baleanu D. Fractional calculus models and numerical methods. World Scientific Publisher Company; 2012.
[20] Caponetto R, Dongola G, Fortuna L, Petras I. Fractional Order Systems and Controls. World Scientific Singapore; 2010.
[21] Oldham KB, Spanier J. the Fractional Calculus. New York: Academic Press; 1974.
[22] Miller KS, Ross B. An introduction to fractional Calculus and Fractional differential equations. NY: John Willey; 1993.
[23] S.G. Samko, A.A. Kilbas, O.I. Marichev, Fractional Integrals and Derivatives: Theory and Applications, New York (1993).
[24] Caputo M, Fabrizio M. A new definition of fractional derivative without singular kernel. Progr Fract Differ Appl 2015;1(2):1–13.
[25] Losada J, Nieto JJ. Properties of a new Fractional derivative without singular kernel, Progr. Fract Diff Appl 2015;1:87–92.
[26] Gao F, Yang XJ. Fractional Maxwell fluid with fractional derivative without singular kernel. Therm Sci 2016;3:71–7.
[27] Abdon A, Baleanu D. New fractional derivatives with nonlocal and non-singular kernel: theory and application to heat transfer model. Therm Sci 2016;18.
[28] Atangana A, Koca I. Chaos in a simple nonlinear system with Atangana-Baleanu derivatives with fractional order. Chaos Solitons Fractals 2016;89:447–54.
[29] Alkahtani BST, Atangana A. Analysis of non-homogeneous heat model with new trend of derivative with fractional order. Chaos Solitons Fractals 2016;89:566–71.
[30] Atangana A, Baleanu D. Caputo-Fabrizio derivative applied to groundwater flow within confined aquifer. J Eng Mech 2016;143:D4016005.
[31] Hristov J. Transient heat diffusion with a non-singular fading memory. Therm Sci 2016;20:757.
[32] Hristov J. Steady-state heat conduction in a medium with spatial non-singular fading memory: Derivation of Caputo-Fabrizio space-fractional derivative with Jeffrey's kernel and analytical solutions. Therm Sci 2017;21:827–39.
[33] Saqib M, Ali F, Khan I, Shiekh NA, Jan SA, Haq S. Exact solutions for free convection flow of generalized Jeffrey fluid A Caputo-Fabrizio fractional model. Alex Eng J 2017. http://dx.doi.org/10.1016/j.aej.2017.03.017.
[34] Butt AR, Abdullah M, Raza N, Imran MA. Influence of non-integer order parameter and Hartmann number on the heat and mass transfer flow of a Jeffery fluid over an oscillating vertical plate via Caputo-Fabrizio time fractional derivatives. Eur Phys J Plus 2017;132:144.
[35] Aziz MA, Yahya AS. Heat and mass transfer of unsteady hydromagnetic free convection flow through porous medium past a vertical plate with uniform surface heat flux. J Theor Appl Mech 2017;47:25–58.
[36] Stehfest H. algorithm 368: numerical inversion of Laplace transforms. Commun ACM 1970;13:47–9.
[37] Tzou DY. Macro to Microscale Heat Transfer: The Behavior. Washington: Tylor and Francis; 1970.